*Journal of Transportation Technologies*, **2012, 2, 150-157**
http://dx.doi.org/10.4236/jtts.2012.22016 Published Online April 2012 (http://www.SciRP.org/journal/jtts)

# Lateral Stability Analysis of Heavy-Haul Vehicle on Curved Track Based on Wheel/Rail Coupled Dynamics

**Kaiyun Wang, Pengfei Liu**
Traction Power State Key Laboratory, Southwest Jiaotong University, Chengdu, China
Email: kywang@swjtu.edu.cn

Received December 16, 2011; revised February 7, 2012; accepted March 1, 2012

## ABSTRACT

Being viewed from the standpoint of whole system, the hunting stability of a heavy-haul railway vehicle on a curved track is investigated in this paper. First, a model to simulate dynamic performance of the heavy-haul vehicle on the elastic track is developed. Secondly, the reason of the hunting motion is analyzed, and a bifurcation diagram for the vehicle on the curved track is put forward to simulate the nonlinear critical speed. Results show that the hunting motion of the heavy-haul vehicle will appear due to the larger conicity, the initial lateral shift and the wheelset angle of attack. With the hunting motion appearing, the lateral shift and force of the wheelset are changed sharply and periodically with a wave of circa 3.6 m. There is obvious difference in the bifurcation diagram between on a curved track and on a tangent track. Relative to the centerline of the track, each vehicle body on the curved track has two stable cycles. As for the curved track with a radius of 600 m and a superelevation of 55 mm, the nonlinear critical speed of the heavy-haul vehicle is 76.4 km/h.

**Keywords:** Hunting; Stability; Curved Track; Heavy-Haul Railway; Coupled Dynamics

## 1. Introduction

Developing heavy-haul railways is one efficient measure to increase the transport volume. However, being restricted to the landform in the heavy-haul railway, there are many sharp curved tracks with the radius ranging from 500 m to 1000 m. When a heavy-haul vehicle is negotiating these curved tracks with low speeds, the phenomenon of the hunting motion, usually taking place on the tangent track, will also appear. Due to the hunting motion on the curved tracks, the interaction force between the wheel and the rail is seriously enhanced, the performance of the negotiation is severely deteriorated, the rail is sharply worn, the rail life is clearly shortened, and even the vehicle will derail on the curved track. So, much attention should be paid to the vehicle hunting motion on the curved track.

Studies on the running stability of the railway vehicle have been performed for almost half of century. The first bifurcation analysis of the free running wheelset was carried out by Huilgol [1] and in this research a hopf bifurcation from the steady state was revealed. The first observation of chaotic oscillations in models of railway vehicles was carried out by True *et al*. [2] and Petersen [3]. Dukkipati [4] developed the mathematical linear models to determine the lateral stability or hunting of North American standard three-piece freight truck on track/roller stands, and the theoretical model results were compared with field test data performed by the Association of American Railroads (AAR). In the meanwhile, using linear models, a comparative study on the dynamic stability and steady state curving behavior of some unconventional railway truck designs was carried out by Dukkipati [5]. Further works demonstrating the hunting stability of high-speed vehicle were carried out by Lee and his team [6,7], including the stability on the tangent track [6] and the stability on the curved track [7]. Lee *et al*. [8] modeled eight degrees of freedom (DOFs) for truck system moving on curved tracks, and it was reported that the critical hunting speeds evaluated by using the eight-DOF system differed significantly from those done by the six-DOF system.

Unfortunately, up to now, there is little study about the lateral stability of the heavy-haul vehicle on the curved track, let alone the stability research based on the coupled model between the vehicle and the track.

Therefore, being viewed from the standpoint of the coupled system presented by Zhai *et al*. [9,10], investigation efforts will be focused on the nonlinear hunting stability of the heavy-haul vehicle on the curved track in this paper. Firstly, a model to simulate the dynamic performance of the heavy-haul vehicle on the elastic track is established. Secondly, the reason of the hunting motion on the curved track is analyzed. Lastly, a bifurcation dia-

 

gram for the vehicle on curved track is put forward to simulate the nonlinear critical speed.

## 2. Dynamic Model of Heavy-Haul Vehicle on Curved Track

A curved track contains three main elements such as radius, cant, and gauge. When a heavy-haul vehicle with full freight passes through the small-radius curved track, the interaction between the wheel and the rail is very serious, as causes the track vibrating obviously. **Figure 1** indicates a measured result [11] of dynamic gauge enlargements on a small-radius curve track. It can be seen from the **Figure 1** that the dynamic gauge enlargement is very clear and the maximum value is close to 3.5 mm.

Therefore, for an analysis on the vehicle dynamic performance, including the stability on the curved track, it is very necessary to take the dynamic vibration of the track into account.

### 2.1. Coordinate Systems

The descriptions of the configuration and the orientation of the railway vehicle on the track are related to the definition of coordinate systems. In order to describe the absolute motion of the heavy-haul vehicle on a curved track, two coordinate systems are needed: the inertial coordinate system and the body fixed coordinate system. Only taking a wheelset on a curved track for an example, the coordinate systems are shown in **Figure 2**, where the inertial coordinate system ($O_i$, $X_i$, $Y_i$, $Z_i$) is located on the center line of the track and can not move with the wheelset, and the wheelset fixed coordinate system ($O_w$, $X_w$, $Y_w$, $Z_w$) is located in the mass center of the wheelset and can move with the wheelset. In addition, the positive directions of $y$ in both systems are toward the inner rail of the curved track or the right rail of the tangent track.

Relative to the inertial system, any of the vehicle body has six DOFs, including three DOFs of transfer motions in longitudinal ($X$), lateral ($Y$), and vertical ($Z$), three

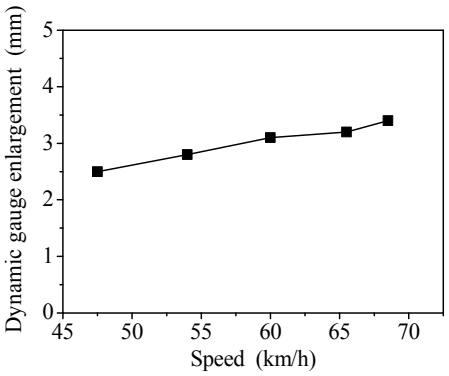


**Figure 1. Measured result of dynamic gauge enlargements on the small-radius curve track.**

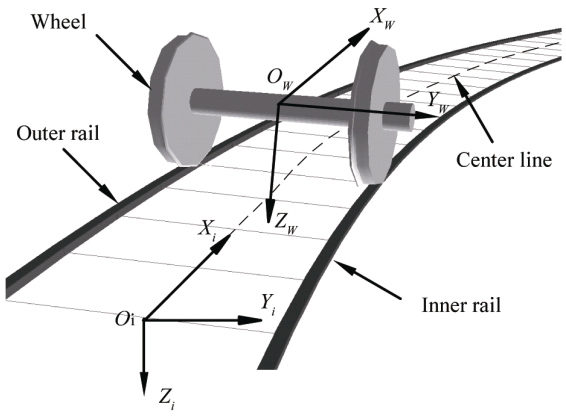


**Figure 2. Coordinate systems on curved track.**

DOFs of a pitch motion ($\beta$), a rolling motion ($\phi$), and a yaw motion ($\psi$). The absolute motion of the body of the vehicle is the vector sum of the transfer and the rotation motions. The relationship between the inertial system and the body fixed system is shown in **Figure 3** [12], in which, p stands any point of a body, the vector $\boldsymbol{r}_p$ ($O_i$, $X_i$, $Y_i$, $Z_i$) in the inertial system stands for its static and spatial position, the vector $\boldsymbol{r}_p$ ($O_B$, $X_B$, $Y_B$, $Z_B$) in the body fixed system stands for its dynamic and spatial position with respect to the inertial system, $\Delta\boldsymbol{r}_c$ is the transfer vector in the body fixed system with respect to the inertial system, and $\Delta\boldsymbol{r}_i$ is the absolute vector of a body.

So, $\Delta\boldsymbol{r}_i$ is calculated by:

$$\Delta\boldsymbol{r}_i = \Delta\boldsymbol{r}_c + \mathbf{A}_B\ \boldsymbol{r}_p - \boldsymbol{r}_p \tag{1}$$

in which, $\boldsymbol{A}_B$ is the rotation matrix in the body fixed system with respect to the inertial system and is formed as following:

$$\boldsymbol{A}_B = \begin{bmatrix} 1 & -\alpha & 0 \\ \alpha & 1 & -\xi \\ 0 & \xi & 1 \end{bmatrix} \begin{bmatrix} 1 & -\psi_B & \beta_B \\ \psi_B & 1 & -\phi_B \\ -\beta_B & \phi_B & 1 \end{bmatrix}$$

where, $\xi$ is the angle difference of two coordinate systems caused by the superelevation (around $X$ axis), $\alpha$ is the angle difference of two coordinate systems (around $Z$ axis), in addition, these parameter values are determined by the line type of the curved track.

According to the Equation (1), all the absolute vectors of vehicle bodies can be calculated. If a body $A$ and a body $B$ are conjoined by a suspension, the relative displacement of the suspension points between $A$ and $B$ is given by:

$$\Delta\boldsymbol{r}_{AB} = \Delta\boldsymbol{r}_B - \Delta\boldsymbol{r}_A \tag{2}$$

in which, the $\Delta\boldsymbol{r}_A$ and $\Delta\boldsymbol{r}_B$ stand for the absolute vector of body $\boldsymbol{A}$ and body $\boldsymbol{B}$, respectively.

Therefore, the relative velocity of the suspension points

 

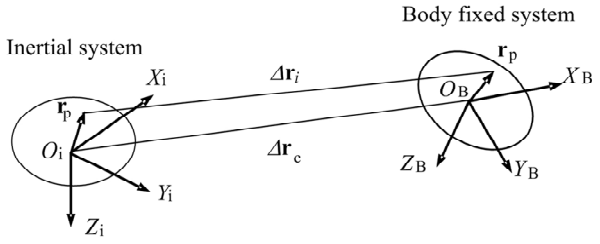


**Figure 3. The vector of body with respect to the inertial system.**

between *A* and *B* is also given by:

$$\Delta \boldsymbol{v}_{AB} = \frac{\mathrm{d}\left(\Delta \boldsymbol{r}_{AB}\right)}{\mathrm{d}t} \tag{3}$$

If the stiffness matrix and the damping matrix in this suspension are $\boldsymbol{K}$ and $\boldsymbol{C}$, respectively**,** the force of the suspension points is calculated as following:

$$\boldsymbol{F} = \boldsymbol{K} \cdot \Delta \boldsymbol{r}_{AB} + \boldsymbol{C} \cdot \Delta \boldsymbol{v}_{AB} \tag{4}$$

## 2.2. Model of Heavy-Haul Vehicle

**Figure 4** shows a three-piece structure of a heavy-haul vehicle which includes two side frames and one bolster. Nowadays, the three-piece structure is widely applied in the heavy-haul vehicle in CR. In order to reduce the unsprung mass, the elastic rubber is set in the axle-box, as is the primary suspension. Apart from this, the components of the structure are similar to those introduced by Xia [13].

The vehicle is modeled as a multi-body dynamic system, as is shown in **Figure 5**. In **Figure 5**, *Z*, *Y* and Φ denote the DOFs of vertical, lateral and roll motions of a component; subscripts *c*, *t* and w represent carbody, side frame and wheelset; subscripts L and R denote the left and right side respectively; $K_{sz}$ and $C_{sz}$ are the vertical stiffness and damping of the secondary suspension; $K_{sy}$ and $C_{sy}$ are the lateral stiffness and damping of the secondary suspension; $K_{pz}$ and $C_{pz}$ are the vertical stiffness and damping of the primary suspension; and $K_{py}$ and $C_{py}$ are the lateral stiffness and damping of the primary suspension.

There are eleven principal components, including one carbody, two bolsters, four side frames, and four wheelsets. It is shown that the carbody is connected to the bolster via the center plates modeled as a spherical joint. Because the radius of the spherical joint is small compared with the other dimensions of the carbody, and the effect of the friction produced by the spherical joint on the roll rotation of the carbody and the bolster is neglected. But the effect of the friction torque on the yaw rotation is still considered. In the secondary suspension, the bolsters are elastically connected to the side frames by springs vertically, and a one-dimension model without

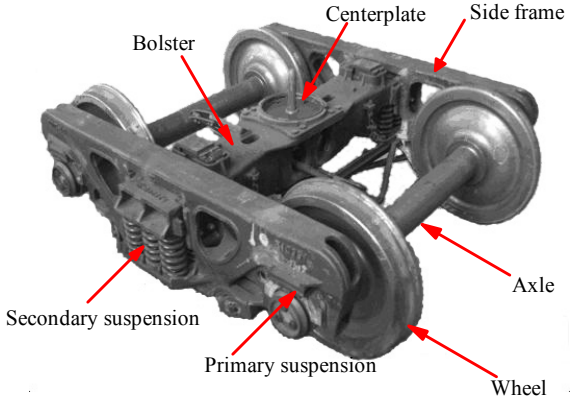


**Figure 4. The construction of the heavy-haul vehicle in CR.**

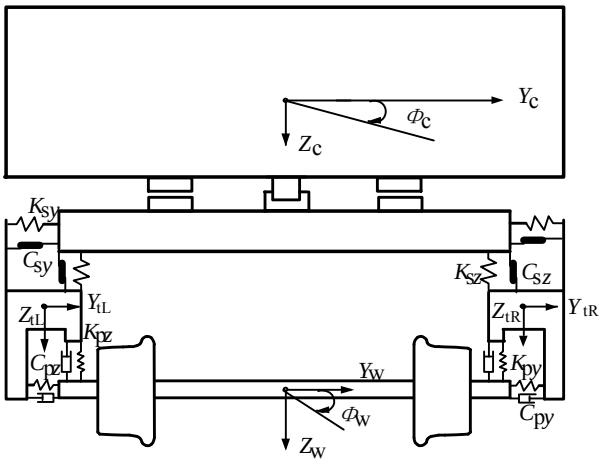


**Figure 5. Description of heavy-haul vehicle dynamics model with end view.**

stick mode is applied to simulate the dry friction in the wedge damper system. The primary suspension is modeled as the parameters of $K_p$ and $C_p$ in longitudinal, lateral and vertical.

All of components are assumed to be rigid. The DOFs of a heavy-haul vehicle are given in **Table 1**, where the total DOFs are 47.

## 2.3. Model of Track

A five-parameter model [9,10] is adopted to model the railway track, as is shown in **Figure 6**. The rail is modeled as a Bernoulli-Euler beam discretely supported at masses. The three layers of discrete springs and dampers represent the elasticity and damping effects of the rail fastening, the ballast, and the subgrade respectively.

## 2.4. Model of the Wheel-Rail Contact

The wheelsets provide the supports for the entire vehicle and supply the contact forces that keep the vehicle system on the track. A new model of three-dimensional geometrical contact between wheel and rail [10,14] is

 

**Table 1. DOFs of a heavy-haul vehicle.**

| Component | Long. | Lat. | Vert. | Roll | Pitch | Yaw |
|---|---|---|---|---|---|---|
| Carbody | - | $Y_c$ | $Z_c$ | $\phi_c$ | $\beta_c$ | $\psi_c$ |
| Bolster ($i$ = 1, 2) | - | - | - | - | - | $\psi_{Bi}$ |
| Front side frame ($i$ = 1, 2) | $X_{tFi}$ | $Y_{tFi}$ | $Z_{tFi}$ | - | $\beta_{tFi}$ | $\psi_{tFi}$ |
| Rear side frame ($i$ = 1, 2) | $X_{tRi}$ | $Y_{tRi}$ | $Z_{tRi}$ | - | $\beta_{tRi}$ | $\psi_{tRi}$ |
| Wheelset ($i$ = 1 - 4) | - | $Y_{wi}$ | $Z_{wi}$ | $\phi_{wi}$ | $\beta_{wi}$ | $\psi_{wi}$ |

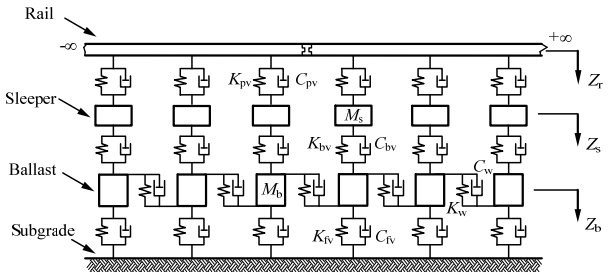


**Figure 6. Description of a five-parameter track model.**

adopted. All the contact parameters are calculated online, including the contact point and its curvature, the conicity, and so on. The normal force of wheel-rail contact is described by a non-linear Hertzian contact theory, and the tangential force is calculated by a Shen-Hedrick-Elkins formula [15].

## 3. Reason of Hunting Motion of Heavy-Haul Vehicle on Curved Track

When a heavy-haul vehicle negotiates a curved track at a low speed, some unbalanced centrifugal forces will appear in the vehicle system due to the multiple effects such as speed, curve radius, superelevation, and so on. Under the action of the unbalanced centrifugal forces, wheelsets will deviate from the track centerline. Both the theoretical and experimental results [11] show that the lateral shifts of wheelsets are bigger than 4 mm usually.

**Figure 7** illustrates the theoretical result of the conicity for the wheel tread of LM and the rail profile of the heavy-haul railway. During the curved negotiation, the lateral shifts of wheelsets are bigger than 4 mm. So the conicity value is more than 0.1, as can help to improve the self-steering ability of the wheelset. It is worth pointing out that the conicity value of the curved track is bigger than the value of the tangent track. In addition, as for the vehicle system on the curved track, the lateral shift is a kind of outside excitation, and the wheelset centerline is not under the radial situation, and the wheelset angle of attack, *i.e.* the angle between the wheelset axis and the radius of the curve, will appear on the wheelset.

Consequently, under the effects of the large conicity,

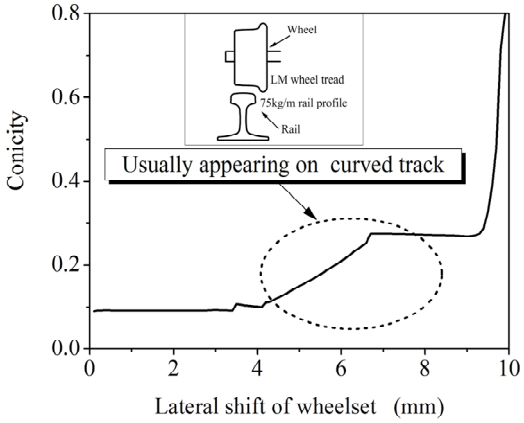


**Figure 7. Conicity versus lateral shift of wheelset.**

the excitation of the lateral shift, and the wheelset angle of attack, the hunting motion appears easily for the wheelsets of a heavy-haul vehicle. Especially for the wagons assembled with the worn components and the worsened suspensions, the hunting stability on curved track is much worse.

Furthermore, a numerical example of the hunting motion of a heavy-haul vehicle with no freight is given, in which, the radius is 600 m, the superelevation of outer rail is 55 mm, the negotiation speed is 85 km/h, the transitions are made of parabolic curves, and other dynamic parameters are evaluated [10,16]. The calculated results of the lateral shift of the wheelset are presented in **Figure 8**, including the time and frequency domain results. It can be seen from **Figure 8(a)** that the phenomenon of the hunting motion appears at the point of spiral to curve, at the point of curve to spiral, and in the whole circular line, and there is lateral and periodic oscillation on the wheelset. Under this situation of the hunting motion, the dominant frequency of the lateral shift is circa 6.5 Hz, as is shown in **Figure 8(b)**.

According to the following formula

$$\lambda = \frac{v}{f} \tag{5}$$

in which, $\lambda$ stands the wave length, $v$ is the vehicle speed, and $f$ is the dominant frequency.

So, the hunting wave length is circa 3.6 m correspondingly, which is quite close to the hunting wave length on a tangent track [17].

**Figure 9** shows the calculated results of the wheelset lateral force under this condition of the hunting motion. It is noticeable that the lateral interaction forces between the wheel and the rail change severely and fluctuate periodically when the phenomenon of the hunting motion of the wheelset appears. The main reason is that, due to the effects of the lateral shift and wheelset angle of attack, the severe impact contact may happen between the root of the wheel flange and the rail side.

 

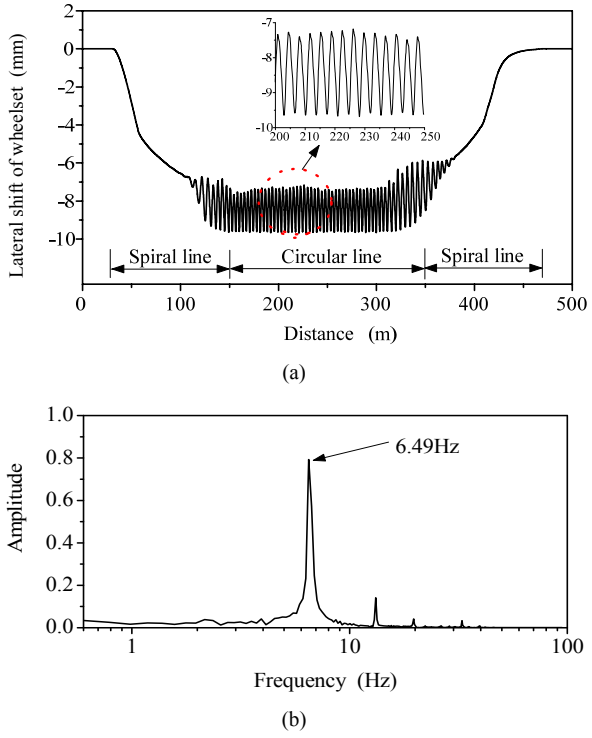


**Figure 8. Calculated results of lateral shift of wheelset on curved track, (a) Response in time domain, (b) Response in frequency domain.**

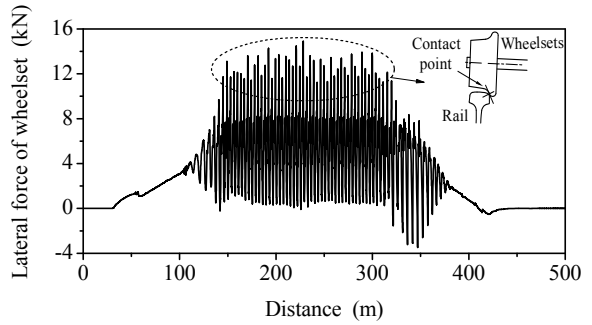


**Figure 9. Calculated results of wheelset lateral force.**

**Figure 10** shows the lateral displacement of outer rail under this case. It can be seen that there is lateral and periodic oscillation on the outer rail during the hunting motion of the wheelset. However, due to the centrifugal forces, the rail will not go back to its resting position.

## 4. Bifurcation Diagram for Heavy-Haul Vehicle on Curved Track

The results [16,17] have proved that once the hunting motion of a vehicle occurs on a tangent track, the wheelset will have a lateral and periodic motion, and there is a stable limit cycle relative to the track centerline. The lateral stability characteristic could be described as an "*S*" shape curve, as is shown in **Figure 11** [2,16,17],

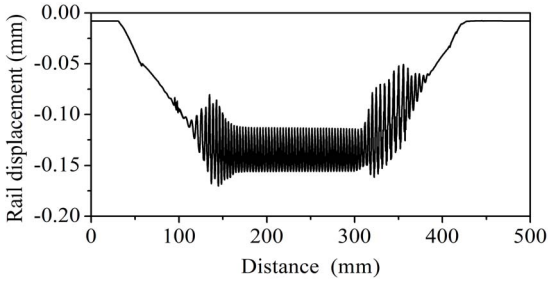


**Figure 10. Calculated results of lateral displacement of outer rail.**

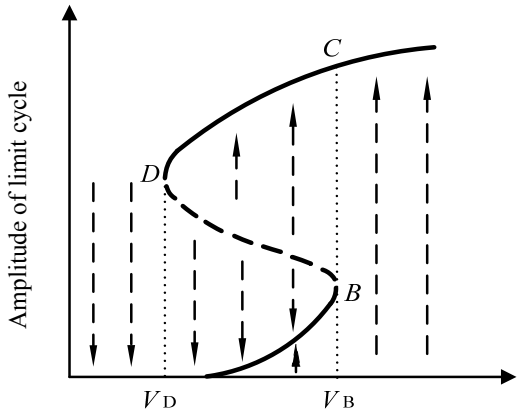


**Figure 11. Typical bifurcation diagram for nonlinear vehicle system on tangent track.**

where the solid line and the dashed line represent the stable and the unstable limit cycle, respectively.

Whereas, according to the calculated results mentioned above, when the hunting motion occurs on a curved track for the wheelset, there is a lateral and periodic oscillation deviating from the centerline of the track. Meanwhile, due to the deviation of the wheelset from the track centerline, two stable limit cycles relative to the centerline of the track can be observed simultaneously, as is shown in **Figure 12**. One stable limit is defined as "large ring", which represents the motion state of the wheelset with the largest amplitude of the lateral shift. The other stable limit is defined as "small ring", which describes the motion state of the wheelset with the smallest amplitude of the lateral shift. Besides, the dashed line in **Figure 12** represents the boundary between the "large ring" and the "small ring".

So, on the basis of the typical bifurcation diagram on tangent track (shown in **Figure 11**) and the motion characteristics on a curved track (shown in **Figure 12**), the bifurcation diagram of nonlinear vehicle system on a curved track can be obtained, as is shown in **Figure 13**, where the solid lines (*CD* and *C′D′*) and the dashed lines (*BD* and *BD′*) also represent stable and unstable limit cycle, respectively, and the horizontal line (*AB*) indicates the equilibrium position of the system deviating from the

 

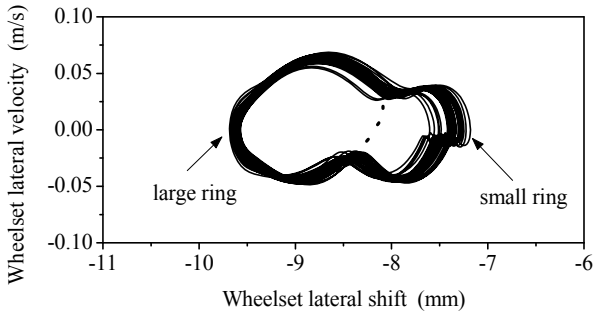


**Figure 12. Wheelset lateral shift versus velocity with hunting motion.**

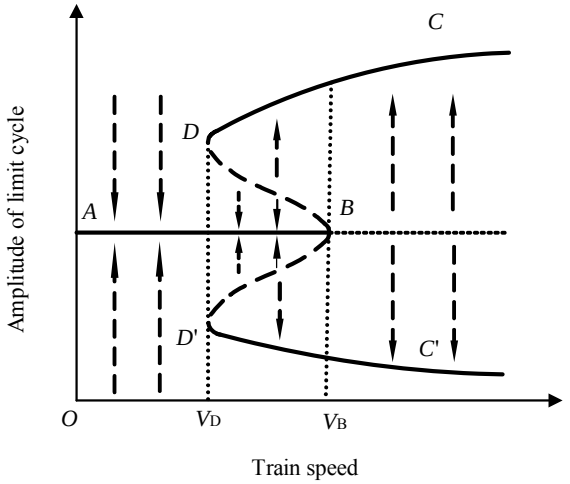


**Figure 13. Bifurcation diagram for nonlinear vehicle system on curved track.**

track centerline.

In **Figure 13**, the abscissa denotes the train speed; the ordinate denotes the amplitude of limit cycle vibration depending on the system disturbances, e.g., the amplitude of the lateral displacement of the leading wheelset. When the train speed $V$ is less than $V_D$, the system vibration will stabilize to the equilibrium position for any external disturbances, as is similar to the diagram on tangent track (shown in **Figure 11**). When the train speed $V$ is larger than $V_B$, two stable limit cycles will be observed no matter what amplitude of the external disturbance is. However, in the interval $V_D < V < V_B$, the situation of system vibration will depend on the amplitude of the external disturbance.

It also can be seen from **Figure 13** that, given an external disturbance with a large disturbance and an initial speed being lower than $V_D$, if the vehicle speed is increased little by little, two stable limit cycles will appear simultaneously when the speed is $V_D$, and the ordinate values at points $D$ and $D'$ are the amplitudes of the limit cycles. On the contrary, given an external disturbance with a large disturbance and an initial speed being higher than $V_B$, if the vehicle speed is reduced step by step, two stable limit cycles will disappear immediately when the speed is $V_D$ and the system vibration will stabilize to the equilibrium position at points $D$ and $D'$.

So, according to the bifurcation diagram for nonlinear vehicle system on the curved track, the speed $V_D$ at points $D$ and $D'$ is called the nonlinear critical speed, and the speed $V_B$ at point $B$ is called the linear critical speed.

## 5. Nonlinear Critical Speed of Heavy-Haul Vehicle on Curved Track

In order to calculate the nonlinear critical speed of a heavy-haul vehicle on a curved track accurately, the points $D$ and $D'$ in **Figure 13** should be found out. Therefore, the "Speed Reducing Method" (SRM) put forward in paper [17,18] is adopted here. It is noticeable that the value of the initial external disturbance should be more than 8mm for a curved track.

Using the SRM, the nonlinear critical speed of a heavy-haul vehicle on a curved track can be calculated. Taking a typical heavy-haul vehicle running on a curved track in CR for an example, the dynamic parameters are the same as those referred above, the radius of the curved track is 600 m and the superelevation is 55 mm. **Figure 14** shows the dynamic response of the lateral shift of the wheelset when the speed is reduced from 140 km/h to 42 km/h gradually. It can be seen from **Figure 14** that, at speeds ranging between 140 km/h and 76.4 km/h, there are the lateral and periodic oscillation on the wheelset and there are two limit cycles with amplitudes of about 10 mm and 7 mm respectively, and when the speed is 76.4 km/h, the lateral shift of the wheelset will stabilize to equilibrium position suddenly. So, it can be deduced that the nonlinear critical speed of the vehicle is 76.4 km/h under these given situations.

On the basis of the research experience and results, Wang [19] has pointed out that the ratio of the nonlinear critical speed to the largest operating speed should be more than 1.2. Consequently, for a curved track with a radius of 600 m and a superelevation of 55 mm, the maximum negotiation speed of this heavy-haul freight

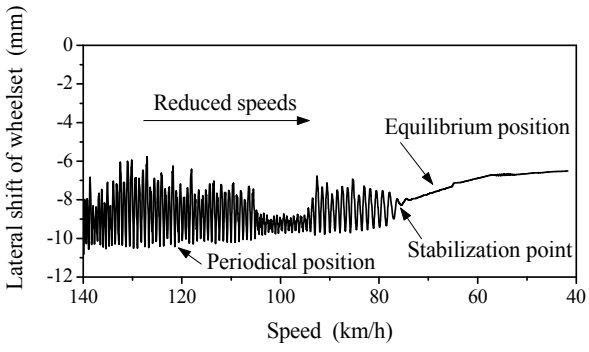


**Figure 14. Wheelset lateral shift versus speeds of heavy-haul vehicle on curved track.**

 

wagon should be 61 km/h. However, according to the code for design of railway line [20], it is prescribed that the maximum negotiation speed of a freight truck on this curved track is 65 km/h. Moreover, the practical operation experience also proves the fact that the negotiation speed usually reaches 65 km/h on this curved track. Thus, when a freight vehicle passes through this curved track with a speed of 65 km/h, the nonlinear critical speed of the vehicle should be more than 76.4 km/h. That is to say, the lateral stability of this type vehicle cannot meet the real requirement for the curved track, and the hunting motion appears usually.

Furthermore, compared with the results in paper [17] that the nonlinear critical speed of this heavy-haul vehicle on a tangent track is 134 km/h, it can be concluded that the nonlinear critical speed of a vehicle on a curved track is lower than that on a tangent track. In other words, the performance of the lateral stability on a curved track is worse than that on a tangent track.

## 6. Conclusions

1) Due to effects of various factors such as the large conicity, the excitation of the lateral shift and the wheelset angle of attack, the hunting motion appears easily when a heavy-haul vehicle negotiates a curved track at a low speed. Under this situation of the hunting motion, there are two stable limit cycles relative to the track centerline, as is different with the phenomenon on a tangent track where there is one stable limit cycle.

2) The nonlinear critical speed of the heavy-haul vehicle on the curved track can be calculated by the SRM. As for the curved track with a radius of 600 m and a superelevation of 55 mm, the nonlinear critical speed of the heavy-haul vehicle is 76.4 km/h, which is lower than the speed on the tangent track.

3) Finally, for the curved track, much attention should be paid to the lateral stability, as well as the running safety.

## 7. Acknowledgements

The authors wish to acknowledge the support and motivation provided by National Natural Science Foundation of China (51075340) and Tong Education Foundation for Young Teachers in the Higher Education Institutions (121075) and Program for Innovation Research Team in University in China (No. IRT1178).

## REFERENCES

[1] R. R. Huilgol, "Hopf-Friedrichs Bifurcation and the Hunting of a Railway Axle," *Quarterly Journal Application Mathematics*, Vol. 36, 1978, pp. 85-94.

[2] T. Hans and K. Petersen, "A Bifurcation Analysis of Nonlinear Oscillation in Railway Vehicles," *Proceeding of the 8th IAVSD Symposium*, Cambridge, 15-19 August 1983, pp. 320-329.

[3] K. Petersen, "Chaos in a Railway Bogie," *Acta Mechanica*, Vol. 61, No. 1-4, 1986, pp. 91-107.

[4] R. V. Dukkipati, "Lateral Stability Analysis of a Railway Truck on Roller Rig," *Mechanism and Machine Theory*, Vol. 36, No. 2, 2001, pp. 189-204. doi:10.1016/S0094-114X(00)00017-3

[5] R. V. Dukkkipati and S. N. Swamy, "Lateral Stability and Steady State Curving Performance of Unconventional Rail Tracks," *Mechanism and Machine Theory*, Vol. 36, No. 5, 2001, pp. 577-587. doi:10.1016/S0094-114X(01)00006-4

[6] S. Y. Lee and Y. C. Cheng, "Hunting Stability Analysis of High-Speed Railway Vehicle Trucks on Tangent Tracks," *Journal of Sound and Vibration*, Vol. 282, No. 3-5, 2005, pp. 881-898. doi:10.1016/j.jsv.2004.03.050

[7] Y. C. Cheng and S. Y. Lee, "Nonlinear Analysis on Hunting Stability for High-Speed Railway Vehicle Trucks on Curved Tracks," *Journal of Vibration and Acoustics*, Vol. 127, No. 4, 2005, pp. 324-332. doi:10.1115/1.1924640

[8] S. Y. Lee and Y. C. Cheng, "Influences of the Vertical and the Roll Motions of Frames on the Hunting Stability of Trucks Moving on Curved Tracks," *Journal of Sound and Vibration*, Vol. 294, No. 3, 2006, pp. 441-453. doi:10.1016/j.jsv.2005.10.025

[9] W. Zhai and X. Sun, "A Detailed Model for Investigating Vertical Interaction between Railway Vehicle and Track," *Vehicle System Dynamics*, Vol. 23, No. 1, 1994, pp. 603-615. doi:10.1080/00423119308969544

[10] W. M. Zhai, K. Y. Wang and C. B. Cai, "Fundamentals of Vehicle-Track Coupled Dynamics," *Vehicle System Dynamics*, Vol. 47, No. 11, 2009, pp. 1349-1376. doi:10.1080/00423110802621561

[11] W. M. Zhai and K. Y. Wang, "Lateral Interactions of Trains and Tracks on Small-Radius Curves: Simulation and Experiment," *Vehicle System Dynamics*, Vol. 44, No. 1, 2006, pp. 520-530. doi:10.1080/00423110600875260

[12] E. C. Slivsgaard, "On the Interaction between Wheels and Rails in Railway Dynamics," Ph.D. Dissertation, Technical University of Denmark, Copenhagen, 1995.

[13] F. Xia, "The Dynamics of the Three-Piece-Freight-Truck," Ph.D. Dissertation, Technical University of Denmark, Copenhagen, 2002.

[14] G. Chen and W. M. Zhai, "A New Wheel/Rail Spatially Dynamic Coupling Model and Its Verification," *Vehicle System Dynamics*, Vol. 41, No. 4, 2004, pp. 301-322. doi:10.1080/00423110412331315178

[15] Z. Shen, J. Hedrick and J. Elkins, "A Comparison of Alternative Creep Force Models for Rail Vehicle Dynamic Analysis," *Proceeding of the 8th IAVSD Symposium*, Cambridge, 15-19 August 1983, pp. 591-605.

[16] W. M. Zhai and K. Y. Wang, "Lateral Hunting Stability of Railway Vehicles Running on Elastic Track Structures," *Journal of Computational and Nonlinear Dynamics*, *Transactions of the ASME*, Vol. 5, No. 4, 2010, pp. 1-9.

 

[17] K. Y. Wang and P. F. Liu, "Characteristic of Dynamic Interaction between Wheel and Rail Due to the Hunting Motion on Heavy-Haul Railway," *Engineering Mechanics*, Vol. 28, No. 1, 2012, pp. 235-239.

[18] P. B. Wu and J. Zeng, "A New Method to Determine Linear and Nonlinear Critical Speed of the Vehicle System," *Rolling and Stock*, Vol. 38, No. 5, 2000, pp. 1-4.

[19] F. T. Wang, "Vehicle System Dynamics," China Railway Press, Beijing, 1994.

[20] GB50090-2006, "Code for Design of Railway Line," China Planning Press, Beijing, 2006.

 